Journal of Sustainability Science and Management
Volume 19 Number 6, June 2024: 1-14
eISSN: 2672-7226

ZEROS OF PARTITION FUNCTION FOR Z_5-SYMMETRIC MODEL ON SQUARE LATTICE-PARTICULAR CASE

NIK AIZAD NIK HASMI[1], SITI FATIMAH ZAKARIA[1]* AND FATIMAH ABDUL RAZAK[2]

[1]*Dynamical Systems and Their Applications Research Unit, Department of Computational and Theoretical Sciences, Kulliyyah of Science, International Islamic University Malaysia, 25200 Kuantan, Pahang, Malaysia.* [2]*Department of Mathematical Sciences, Faculty of Science and Technology, Universiti Kebangsaan Malaysia, 43600 Bangi, Selangor, Malaysia.*

**Corresponding author: fatimahsfz@iium.edu.my*
http://doi.org/10.46754/jssm.2024.06.001
Submitted final draft: 14 November 2023 *Accepted: 18 November 2023* *Published: 15 June 2024*

Abstract: We study a statistical mechanics model of multiple-phase transitions called the Z_Q-symmetric model on the square lattice for five possible spin directions (Q = 5). This study aims to investigate the existence of phase transition(s) and discuss the distribution of partition function zeros on the complex-temperature plane. Some cases of energy list χ are considered where they are written in an arbitrary arrangement of integer numbers (usually in decreasing value due to the angle of separation). The partition functions are computed using a transfer matrix approach, and their zeros are found numerically using the Newton-Raphson method. A Monte-Carlo Metropolis simulation is then performed to study the critical point of phase transition. The results are compared to the zeros distribution of the partition functions for the considered cases. Studying this generalised model is vital to mimic the system in the real world and to help experimental works use a more sustainable approach.

Keywords: Z_Q-symmetric model, phase transition, Monte-Carlo simulation, sustainable approach.

Introduction

Mathematical models within statistical mechanics are extensively studied with the critical phase transition point. The simplest model of two states called the Ising model (Ising, 1925), was solved by Onsager (1944). This was generalised by the Q-state Potts model (Potts, 1952) to study models with more spin states. In this paper, we focused on a model represented by integer numbers called the Z_Q-symmetric model, originally investigated based on the angle of separation between the spin states by Martin (1991). The Q in both models represent the number of states under investigation. Here, further model modification was made to explore and understand more about the model by arranging the spin state in arbitrary order.

The Z_Q-symmetric model is also related to the clock model as both are represented on a general discrete planar model where the spin takes one of the Q possible values distributed around the clock-like circle. The model was previously studied by (Martin, 1991; Zakaria, 2016; Zakaria & Manshur, 2019; Manshur *et al.,* 2020) on square and triangular lattices for 5 and 6 possible states. Here, we are focusing on the study for the case of Q = 5, that is, five (5) spin states to determine the existence of phase transition(s) for the model. To date, researchers have managed to obtain exact solutions for the one-dimensional (1D) and two-dimensional (2D) Ising models, thanks to the ground-breaking work of physicists such as Lars Onsager (Onsager, 1944). Obtaining exact solutions for higher dimensions and more complex models is challenging due to increased system complexity. As a result, approximation methods like renormalisation group, mean-field theory techniques and Monte Carlo simulations are utilised to study the system.

Here, we used the finite-size scaling technique to approximate the partition function for the model and then find the zeros distribution of the partition functions. This approach enables us to analyse the systems' phase transition and critical behaviour. Fisher's (1967) and Kadanoff's (1966) works are notable early papers that laid the groundwork for finite-size scaling. Fisher (1965) was also among the earliest to study the complex-temperature zeros of partition function. Later, Yang and Lee (1952) discovered that the zeros lie on a circle in the complex plane, known as the Yang-Lee circle theorem. The properties of these zeros, such as their distribution and behaviour near critical points, provided insights into the nature of phase transitions.

To investigate the critical point further, we used Monte Carlo Metropolis (MCM) simulation for higher lattice size as it often provides approximate results faster than other numerical methods. The efficiency is notable for the model as it is quite complex and deterministic calculations are time-consuming. The MCM method leverages random sampling techniques to explore the parameter space and generate statistical data, allowing for faster data generation than exhaustive computational approaches. Metropolis *et al.* (1953) developed these statistical sampling techniques inspired by games of chance as the scientists then faced complex mathematical calculations to build the atomic bomb through the Manhattan Project.

For the Z_Q-symmetric model, previous work (Zakaria, 2016; Zakaria & Manshur, 2019; Manshur *et al*. (2020) suggested that the emergence of multiple linear curves on the complex temperature plane could predict the existence of multiple phase transitions. Here, we extended the study of Z_Q-symmetric model for $Q = 5$ with arbitrary energy lists χ to offer further validation regarding the existence of the multiple phase transitions for the Z_Q-symmetric model. We studied the zeros of the partition function for the model with increasing lattice sizes on a square lattice and simulated the model using the MCM method to examine the existence of phase transition(s) and to estimate the critical temperature(s) T_c for the model. We compared the observation from the zeros of the partition function with the result of the MCM simulation.

Preliminaries

Here, we present some fundamental concepts that serve as the building blocks for our research and are vital for comprehending the subsequent sections and interpreting the findings.

We take some definitions from the graph theory. It is used to represent our system where the vertices characterise the position and the state of atoms while the edges illustrate the interaction of the sites. The model is defined on a square lattice, one of the seven lattices known as the Bravais lattice, on a 2D crystalline system (Shackelford, 2000). The lattice for our system has specific boundary conditions (bc).

Definition 1 *(Diestel, 2006). A directed graph is a triple* $\Lambda = (V, E, f)$. *The* V *and* E *are set where the elements* $v \in V$ *are called the vertices and the elements* $e \in E$ *are called edges. The* f *is a function* $f : E \to V \times V$. *Given* $e \in E$ *and* $u, v \in V$, *the images* $f(e) = \langle u, v \rangle$ *give the 'source' and 'target' vertex of edge* e. *The distance* $d(u, v)$ *is the number of edges in the shortest path from* u *to* v. *Two vertices* u *and* v *are called nearest neighbours if* $f(e) = \langle u, v \rangle$ *for some* $e \in E$ *i.e., when* $d(u, v) = 1$.

Definition 2 *(Zakaria & Manshur, 2019). Consider a set of lattice sites, a d-dimensional lattice is formed from each side of the nearest neighbours. There is a discrete variable* $\sigma_v \in \{1, 2, ..., Q\}$ *for each lattice site* $v \in V$ *representing the spin of the site. We define the position of the site as* $\sigma_v \in (i \mid i \in \{1, 2, ..., n\})$ *where* $n = |\Lambda|$. *A spin configuration* $\sigma^{(i)} = \sigma = (\sigma_v(1), \sigma_v(2), ... ,\sigma_v(n))$ *is an assignment of spin value to each lattice site. The coordinate function also can be defined based on the dimension of the lattice as* $\sigma_v = (i, j, ...)$ *where* $i, j, ... \in \mathbb{Z}^+$.

Definition 3 *Consider a graph* $\Lambda = (V, E, f)$ *on* $M \times N$ *lattice such that* $M, N \in \mathbb{N}$. *Let the set of vertices* $V = V_I \cup V_B$ *where we call the elements of* V_I *as inner sites and elements of* V_B *as boundary sites such that;*

$$V_B = \left\{ \begin{matrix} \sigma_v(1,1), \sigma_v(2,1), \dots, \sigma_v(M,1), \\ \sigma_v(1,2), \sigma_v(1,3), \dots, \sigma_v(1,N), \\ \sigma_v(M,2), \sigma_v(M,3), \dots, \sigma_v(M,N), \\ \sigma_v(2,N), \sigma_v(3,N), \dots, \sigma_v(M-1,N) \end{matrix} \right\} \text{ and } V_I = V/V_O.$$

Boundary condition defines the edges for the pair boundary sites $u,v \in V_B$. Open bc is defined as no edge that exists for the pair boundary sites, while the pair boundary sites with an edge are called periodic bc. M x N' denote an M by N lattice with open horizontal bc and periodic vertical bc.

Definition 4 *Let G, G′ be two lattice graphs. For the union of two graphs* $G \cup G'$, *we have;*

$$V_{G \cup G'} = V_G \cup V_{G'}$$

and

$$E_{G \cup G'} = E_G \cup E_{G'}$$

where $E_G \cap E_{G'} \neq \emptyset$.

Definition 5 A physical observable O is a measurable quantity or property of a physical system that can be observed or measured experimentally, providing information about the behaviour, characteristics, and interactions of the system. It includes magnetisation, susceptibility, energy, and specific heat.

Materials and Methods

The Z_Q-symmetric model is a model of discrete variables representing the magnetic dipole moment of the atomic spins. The details of the construction of this model are presented by Zakaria (2016).

Without loss of generality, few assumptions and simplifications are made to ease the computation. This model uses a canonical ensemble, where the system can exchange energy with a heat bath at a specific temperature, but other properties will be fixed (Eastman, 2018). It also neglects the external magnetic field, only considering nearest neighbour interaction and every nearest neighbour has a similar interaction strength J. We are interested in studying the ferromagnetic material where the atoms of the material favour alignment as the temperature of the system decreases. Hence, we only considered positive interaction strength. We also set the Boltzmann constant k_B to 1 to ease the computation. So, the inverse temperature β can be defined as $\beta = \frac{1}{T}$. The total energy of the system is given by the Hamiltonian as follows:

Definition 6 The Hamiltonian H of the Z_Q-symmetric model is defined as;

$$H_\chi = -J \sum_{\langle i,j \rangle} \sum_{r=1}^{\left|\frac{Q}{2}\right|} \gamma_r \cos\left(\frac{2\pi r(\sigma(i) - \sigma(j))}{Q}\right) + \gamma_r' \quad (1)$$

$$= -J \sum_{\langle i,j \rangle} \chi[\sigma(i) - \sigma(j)] \quad (2)$$

$$= -Jh \quad (3)$$

where $h = \sum_{\langle i,j \rangle} \chi[\sigma(i) - \sigma(j)]$.

The $\left|\frac{Q}{2}\right|$ represent floor division for $\frac{Q}{2}$ and $\gamma_r, \gamma'_r \in \mathbb{R}$ are the model parameters fixed for a given model. Using rescaling factor γ_r, γ'_r enable us to calculate the Hamiltonian based on energy list χ as in the Equation (2). The energy list χ is defined based on the angle separation between states at site i and site j. The element of χ can be represented as;

$$\chi = \left(\chi[0], \chi\left[\frac{\theta}{Q}\right], \dots, \chi\left[\frac{\left(\left|\frac{Q}{2}\right| + 1\right)\theta}{Q}\right] \right)$$

where

$$\chi[0], \chi\left[\frac{\theta}{Q}\right], \dots, \chi\left[\frac{\left(\left|\frac{Q}{2}\right| + 1\right)\theta}{Q}\right] \in 0 \cup \mathbb{N}.$$

Previous studies considered cases where $\chi[0] > \chi[1] \geq \cdots \geq \chi\left[\frac{[Q]}{2}\right]$ with $\chi\left[\frac{[Q]}{2}\right] = 0$.

Here, we covered some cases that discard the restriction to provide generality for the model. We select particular cases where $\chi[0] < \chi[1]$. The partition function for this model is defined as follows:

Definition 7 The partition function Z of the Z_Q-symmetric model is defined as;

$$Z_\chi(\beta) = \sum_{\sigma \in \Omega} \exp\left(-\beta H \chi(\sigma)\right) \quad (4)$$

$$= \sum_{\sigma \in \Omega} \exp(\beta J h) \quad (5)$$

where Ω is a set for all configurations σ_k for graph Λ.

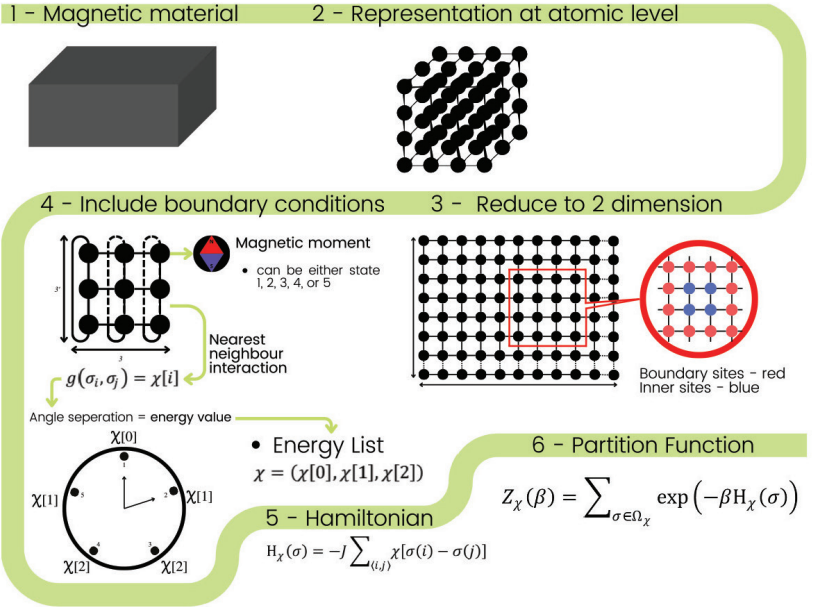

Figure 1: Flowchart of the construction of the Z_5-symmetric model starting from the physical material, its representation on the finite square lattice with specific boundary conditions, the definition of the sites and edges of the system to the main equation (partition function)

The choice of boundary conditions is open horizontal bc and periodic vertical bc chosen to expedite the computation of the partition function Z for each case. The flowchart visualisation of the study of the Z_5-symmetric model and the lattice are described in Figure 1.

The list of cases considered is presented in Table 1, where the highlighted cases are the new cases. We rerun some cases examined by Zakaria (2016) for validation. Both (3, 1, 0) and (3, 2, 0) are chosen as Zakaria (2016) suggested some relation of those two models from their energy step. The energy step is the difference for the consecutive energy value $\chi[i]$. Two new particular models are chosen by swapping the first and the second elements of the models. The cases with lattice sizes 10 x 10', 30 x 30', 50 x 50', 70 x 70', and 100 x 100' are studied for their MCM simulation, while the other cases are studied for the zeros of the partition function.

Computation of Zeros of Partition Function Z

The partition function is computed for each configuration of the cases where $|\Omega| = (M \times N)^Q$. For simplicity, we calculated h as defined in Definition 6 and let $x = e^{BJ}$ so that

$$Z(x) = \sum_{\sigma\in\Omega} x^h. \quad (6)$$

is in polynomial form. For $Z(x) = 0$, the zeros on the complex Argand plane are approximated using the Newton-Raphson (NR) method.

The time taken to calculate partition function Z as lattice size grows increases significantly as $|\Omega|$ increases exponentially. Hence, Zakaria (2016) and Manshur *et al.* (2020) use a transfer matrix approach to expedite the computation.

Let graph $\Lambda \subset \Gamma$ be a lattice with size M x 2' such that the sites at the $N = 2$ do not have vertical edges and graph $\Lambda' \subset \Gamma$ is a lattice with a size 1 x 1'. Hence, we can get our desired graph Γ that has size $M \times N$ by performing the union of graphs $\Lambda^{N-2}\ \Lambda'$ for $N > 1$.

We represented the partition function Z in matrix form. The entries of a matrix are indexed as ij where i is the position of the entry's row and j is the position of the entry's column. We

Table 1: Z_5-symmetric models with their respective energy list and size

χ	Lattice Size									
(3,1,0)	5 x 5'	6 x 6'	7 x 7'	8 x 8'	9 x 9'	10 x 10'	30 x 30'	50 x 50'	70 x 70'	100 x 100'
(3,2,0)	5 x 5'	6 x 6'	7 x 7'	8 x 8'	9 x 9'	10 x 10'	30 x 30'	50 x 50'	70 x 70'	100 x 100'
(1,3,0)	5 x 5'	6 x 6'	7 x 7'	8 x 8'	9 x 9'	10 x 10'	30 x 30'	50 x 50'	70 x 70'	100 x 100'
(2,3,0)	5 x 5'	6 x 6'	7 x 7'	8 x 8'	9 x 9'	10 x 10'	30 x 30'	50 x 50'	70 x 70'	100 x 100'

arrange one-to-one x^h to the entries of a square matrix T. The matrix index ij corresponds to ij in $\sigma(i, j)$. Instead of using ij = 1, 2, ..$\mathbb{Z}$ for the matrix index, we index the matrix based on the configurations of the lattice such that;

$$i = \left(\sigma_1, \sigma_2, \dots, \sigma_{\left|\frac{\Omega}{2}\right|}\right)$$

and

$$j = \left(\sigma_{\left|\frac{\Omega}{2}\right|+1}, \dots, \sigma_{\left|\frac{\Omega}{2}\right|-1}, \sigma_{|\Omega|}\right).$$

We can define the transfer matrix as

$$\mathrm{T}_{ij} = Z_{\Gamma}^{\Lambda}. \quad (7)$$

Transfer matrix for the graph Λ' is called a special case transfer matrix as x^h are arranged in the matrix diagonally, i.e., $i = j$.

Based on the Chapman-Kolmogorov theorem (Papoulis & Pillai, 2011), the summation of the product of partition vectors for graph Λ and Λ' can produce the partition function of a new combined graph ΛΛ' (Zakaria & Manshur, 2019). Hence, we can get the partition function Z_Γ by performing the multiplication of the transfer matrix multiple times, i.e., $Z_\Gamma = Z_\Gamma^{\Lambda^{N-2}} Z_\Gamma^{\Lambda'}$ for $N > 1$.

Monte Carlo Simulation

We employed the Metropolis algorithm (Kotze, 2008) further to investigate the existence of the phase transition critical point. It involves iteratively updating the system's configuration by randomly flipping a site to a randomly chosen state and accepting or rejecting these changes based on a Metropolis acceptance criterion. The new configuration is accepted if it has higher magnetisation than the old configuration. If it has lower magnetisation, it will be accepted if a randomly generated real number that ranges from 0 to 1 is lower than the Boltzmann factor $e^{\beta\Delta M}$ where β is the inverse temperature and ΔM is the magnetisation difference between the new and old configuration. The Boltzmann factor ensures that the Monte Carlo simulation samples state in accordance with their relative probabilities at a specified temperature. We used random flipping to ensure all possible configurations were explored for sufficient iterations. This can help to capture critical fluctuation. The probability of choosing a new state is equal for all states to avoid unbiased sampling. This also represents the symmetry of the model.

The system is initialised in the simulation by a random configuration to the lattice. The simulation is then performed for 10,000 iterations for a temperature T to ensure the system reaches equilibrium. Then, another 10,000 iterations are performed where the equilibrium lattice is now assigned as the initial lattice. During sampling iterations, the data is calculated for each configuration to find the statistical measures for each T to get the observables (total energy, specific heat, magnetisation, and susceptibility) value and graphed over T. Using 10,000 iterations

for the sampling process can ensure the statistical independence of the sampled configurations.

Here, we presented the system using increasing lattice sizes and the 100 by 100' lattice size as the highest, considering our time, computing resources, and minimising the finite boundary effect. This simulation was simulated using decreasing temperature. By starting from a high temperature and gradually reducing it, the system has a higher probability of exploring different configurations and overcoming energy barriers to reach equilibrium. The temperatures were defined by a consistent decrement of 0.01 to ensure the smoothness of the graph.

For magnetisation, we defined nearest neighbour atoms with similar states to have the value 1 while nearest neighbour atoms with different states give a 0 magnetisation value. We then stored the multiplicity of each magnetised interaction to imitate the magnetic region of the ferromagnetic system. The mean of the multiplicities calculated the magnetisation value.

Other observables are susceptibility and specific heat. Both susceptibility and specific heat refer to the reactiveness of the system to the external field. However, our system neglects the magnetic field and has already reached equilibrium with the heat bath. So, we used the fluctuation-dissipation theorem to calculate both observables. This theorem states a general relationship between the response of a given system to an external disturbance and the internal fluctuation of the system in the absence of the disturbance (Kubo, 1966). It relates the equilibrium fluctuations of a physical quantity to its response function, which describes how the system reacts to small changes in an external parameter. This theorem is influenced by the work of Einstein on Brownian motion (Einstein, 1905). He derived a relation between the mean square displacement of a particle undergoing random motion (related to fluctuations) and its mobility (related to response) in a fluid. This theorem is fundamental to the statistical mechanics of nonequilibrium states or of irreversible processes in general (Kubo, 1966).

Here, we used the variance of the magnetisation and the variance of the total energy as the correlation function for susceptibility and specific heat, respectively. Hence, we can define susceptibility as $\chi s = \beta[Var(M)]$ and specific heat as $C_v = \beta^2[Var(E)]$ (Kotze, 2008). The variance of the observable gives information about the dispersion of the configurations of the system at a temperature, while the inverse temperature β scales the difference with respect to temperature.

The fact that the observables change over time hints at the existence of phase transition. In addition, sudden changes in the graph can indicate the occurrence of phase transition in the system. We know that the sudden change may also be caused by other factors such as crossover, a change in the dominant interactions, or multiple competing phases. Thus, we compared the observed sudden change with the observation of the zeros of the partition function.

Results and Discussion

Zeros of Partition Function

In this section, we present the graph of the zeros of the partition function in the complex-Argand plane for all considered cases. We analysed the locus of the zeros based on their thickness, indication of approaching the real axis, the distance from the real axis, and the possibility of merging or branching out. The real axis $(-\infty, 0)$-region is not physical as the temperature is negative. The ferromagnetic material which has interaction energy $J > 0$ can be studied over the real axis $(1, \infty)$-region. The $(-\infty, 0)$-region and $(0, 1)$-region are not physical as the zeros $x = e^{BJ}$ and the temperature T are both negative. Note that the $(0, 1)$-region represents the antiferromagnetic material when interaction energy $J < 0$. Here, we focused on the $(1, \infty)$ -region for the study of ferromagnetism.

We analysed the zeros distribution of the partition function based on the Lee-Yang theorem. Lee and Yang (1952) showed that the equation of states of phase transition is closely related to the root distribution of the partition function. Lee-Yang's theorem states

that the roots always lie on a circle under certain conditions. Hence, we examined the locus of zeros, which indicates they will cut the real axis. The point where the loci cut the real axis can give us a temperature value that is considered a critical temperature T_c. Thus, the system undergoes a phase transition at that temperature. Figures 2 through 5 present the distribution of the zeros for the partition function of $\chi = (3, 1, 0)$, $(3, 2, 0)$, $(1, 3, 0)$, $(2, 3, 0)$.

Refer to Figure 2. The zeros distribution of the partition function $Z_{(3, 1, 0)}$ formed a visible arc near the positive real axis. As lattice size increases [Figure 2 (a)], the zeros become dense and move closer to the real axis. The change of the end points closest to the positive real axis specifically in the $(1, \infty)$ range indicates that the increase in size gives better observation and as the lattice size increases to the thermodynamic limit, this closest point is expected to reach the real line axis. The locus from the zeros will be smooth and cut the real axis at the phase transition critical point. This case has been reproduced based on the work by Zakaria (2016), which shows that it has only one (1) curve, which indicates a single-phase transition temperature. Figure 2 (b) presents the distribution of the zeros for the largest even cases that have been considered in this paper. The even case has a smooth arch compared to the odd cases, as it is less affected by the small lattice size and the choice of boundary condition.

Figure 3 presents the zeros distribution of the partition function for $Z_{(3,2,0)}$. This figure suggests that multiple loci of zeros may approach the real axis as the lattice size increases. Some loci close to each other may converge to form a dense single arc as they grow to the thermodynamic limit. The zeros that form another curve far from the dense one may be smooth out as the size increases. Nevertheless, they are still far from the real axis. Again, the even case has a smooth arch compared to the odd cases, as it is less affected by the small lattice size and the choice of boundary condition.

The zeros distribution of the partition function for $Z_{(1,3,0)}$ is shown in Figure 4. Similar to the previous cases, a clear arc is approaching the real axis as the lattice size increases. However, there is a visible finite size effect for this case where some of the zeros for the even N case are smoother than the odd N case. The even N case indicates the existence of a single locus of zeros or single-phase transition. Some zeros in the odd N case have values outside of the dense locus (outliers), which suggests this finite size effect.

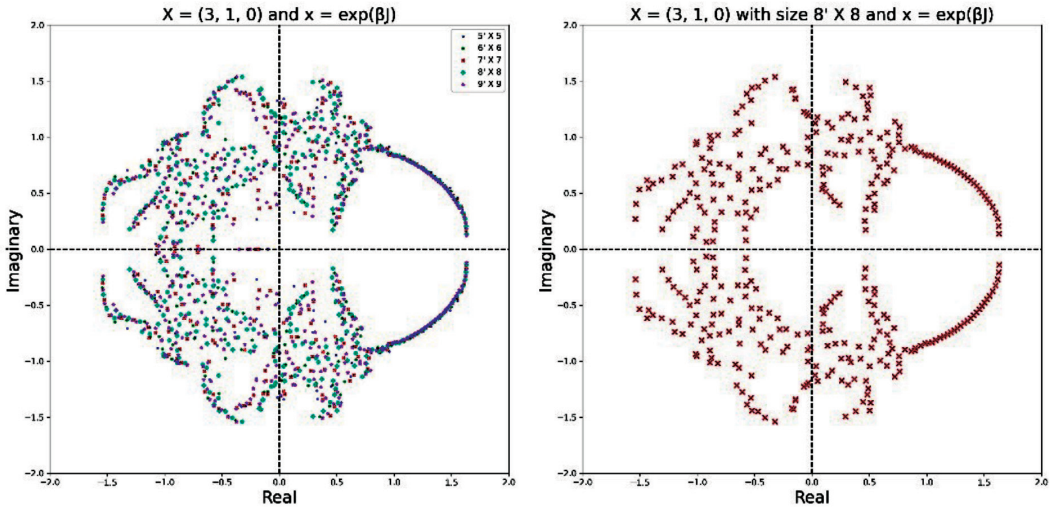

(a) (b)

Figure 2: Zeros distribution of $Z_{(3,1,0)}$ for lattice size (a) from 5 × 5' to 9 × 9' and (b) 8 × 8'

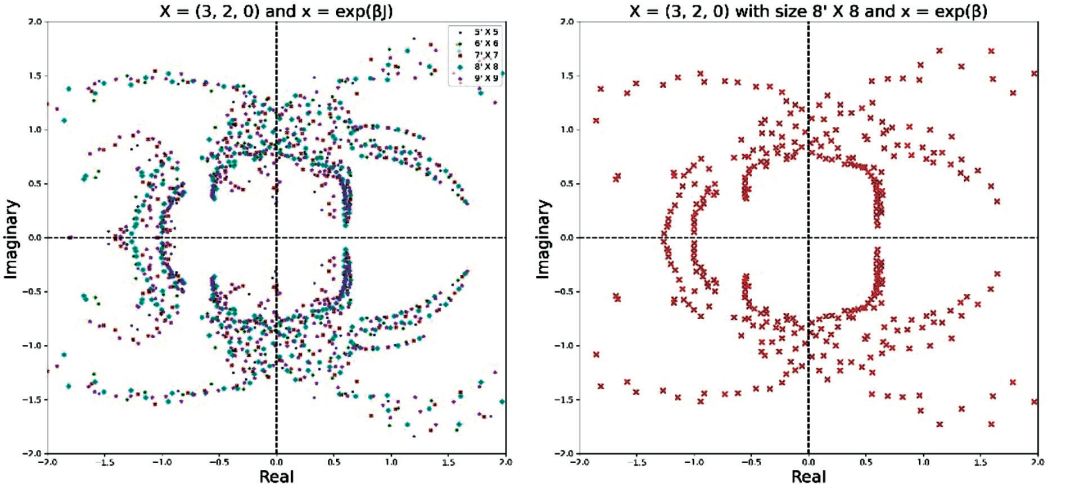

(a) (b)

Figure 3: Zeros distribution of $Z_{(3,2,0)}$ for lattice size (a) from 5 × 5' to 9 × 9' and (b) 8 × 8'

From Figure 5, the zeros of the partition function for $Z_{(2,3,0)}$ hints at two arcs approaching the real axis even though they are far from the real axis. Those arcs are more visible for even N. One arc is dense but far from the real axis, while the other arc is thin and dissipates as it approaches zeros. They may converge as N increases. The closest zero to the real axis for $Z_{(3,1,0)}$ and $Z_{(3,2,0)}$ is the zero from lattice 9 by 9' while for $Z_{(1,3,0)}$ and $Z_{(2,3,0)}$ is the zero from lattice 8 by 8'.

In general, the zeros of the partition function for each model show a similar pattern with increasing zeros as the lattice size increases. As lattice size increases, the arcs approaching the real axis will form a line that intersects the real axis at the thermodynamic limit. The intersection is the critical point for the model. In some cases, the emergence of additional loci for odd M is due to the boundary conditions. Even the closest zeros to the real axis of the loci of interest for some models are at even lattice size

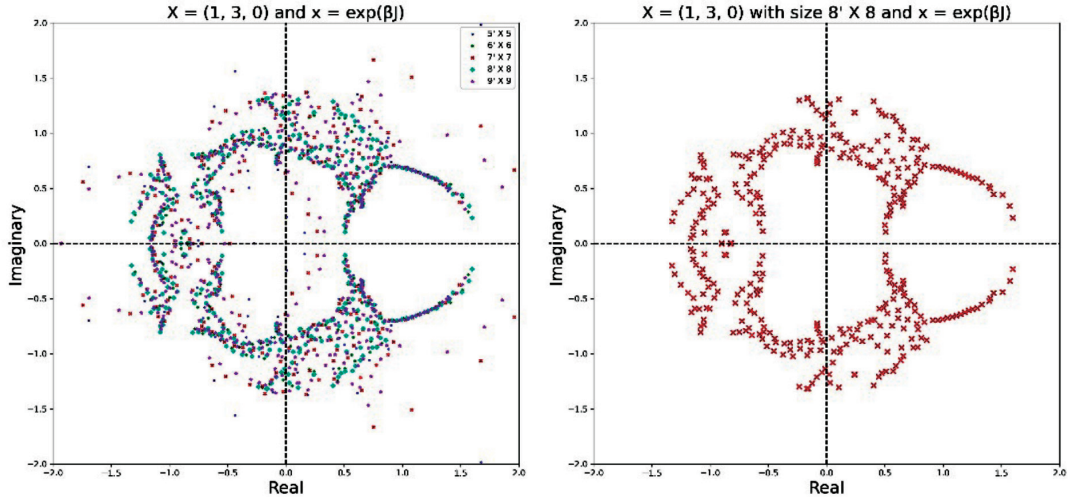

(a) (b)

Figure 4: Zeros distribution of $Z_{(1,3,0)}$ for lattice size (a) from 5 × 5' to 9 × 9' and (b) 8 × 8'

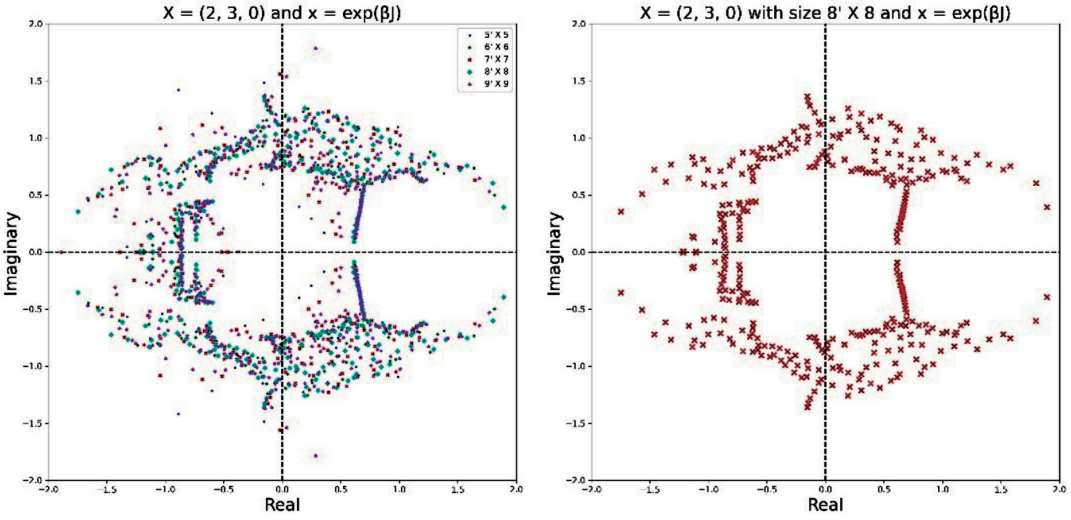

(a) (b)

Figure 5: Zeros distribution of $Z_{(2,3,0)}$ for lattice size (a) from 5 × 5' to 9 × 9' and (b) 8 × 8'

M. However, the boundary effect will vanish at the thermodynamic limit as the ratio of the boundary vertices over inner vertices approaches zero as the lattice size increases.

Observables

The MCM simulation sampled the observables, *0* of the model in the range [0.5, 2.5]. This range was chosen based on the observation from the zeros of the partition functions. For each model, we graphed the total energy *h* per spin, specific heat C_V, magnetisation M_v per spin, and susceptibility χ_s over decreasing temperature. Refer to Figures 6 through 9.

Figure 6 shows the observables for the model (3, 1, 0). Both magnetisation per spin and energy *h* per spin increase logarithmically as temperature decreases. As the lattice size increases, both observables become more stable and less steep. The graph for specific heat and susceptibility is also more prominent as the lattice size increases. The observables for models (3, 2, 0) and (2, 3, 0) also show similar behaviour to the model (3, 1, 0). This can be seen in Figure 7 and Figure 8, respectively. However, the observable for the model (1, 3, 0) as shown in Figure 9 demonstrates different behaviours. The energy per spin for this model decreases as the temperature decreases.

Overall, the magnetisation per spin graph for all cases we studied showed a similar pattern, as shown in Figure 10. Here, we can construe that our MCM simulation results are valid as they were consistent, although they were run separately. However, the susceptibility graphs across models were incoherent. This will be investigated further for future research.

The number of edges for the square lattice with open horizontal bc and periodic vertical bc is given by $N(2M - 1)$. As the temperature decreases, the total energy should be approaching $N(2M - 1) \times \chi[0]$. The model (3, 1, 0) and (3, 2, 0) both have the highest energy for $\chi[0]$. Hence, the total energy should increase, approaching 19,900 × 3 = 59,700 considering the $M, N = 100$. The highest total energy *h* for the model (2, 3, 0) and the model (1, 3, 0) are 39,800 and 19,900 respectively. These models first energy list $\chi[0]$ is lower than $\chi[1]$ and higher than $\chi[2]$. Thus, the total energy *h* may increase or decrease as temperature decreases. From the result (Figure 8 and Figure 9), the total energy *h* of the model (2, 3, 0) increases while the total energy *h* of the model (1, 3, 0) decrease as the temperature decreases.

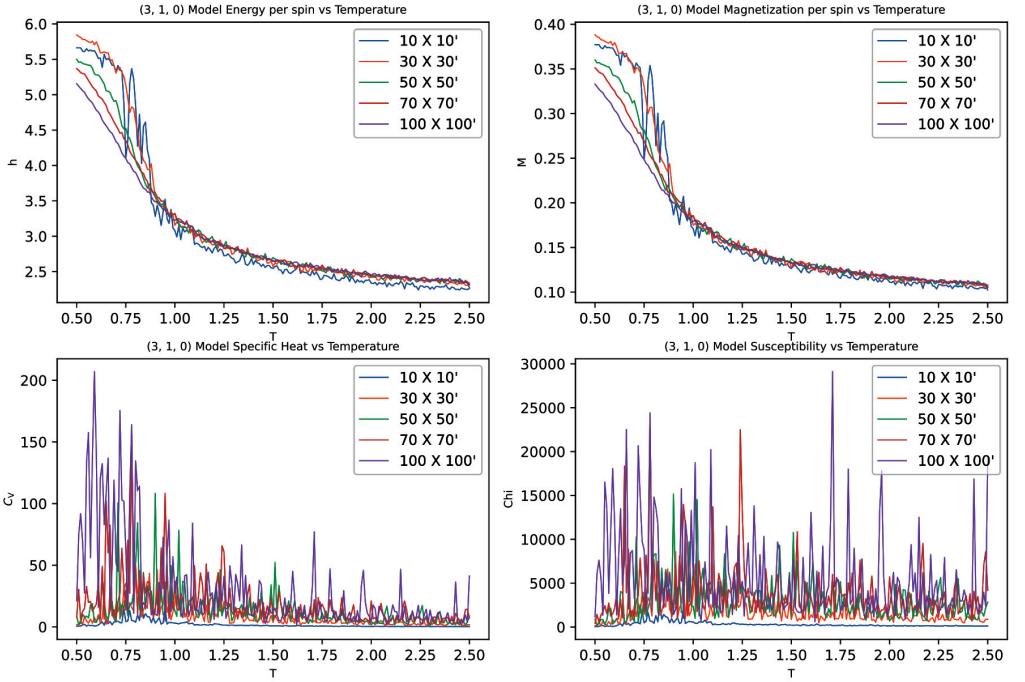

Figure 6: Graphs of observables $\langle O \rangle_{(3,1,0)}$ over temperature T for lattice size 10 × 10', 30 × 30', 50 × 50', 70 × 70' and 100 × 100'

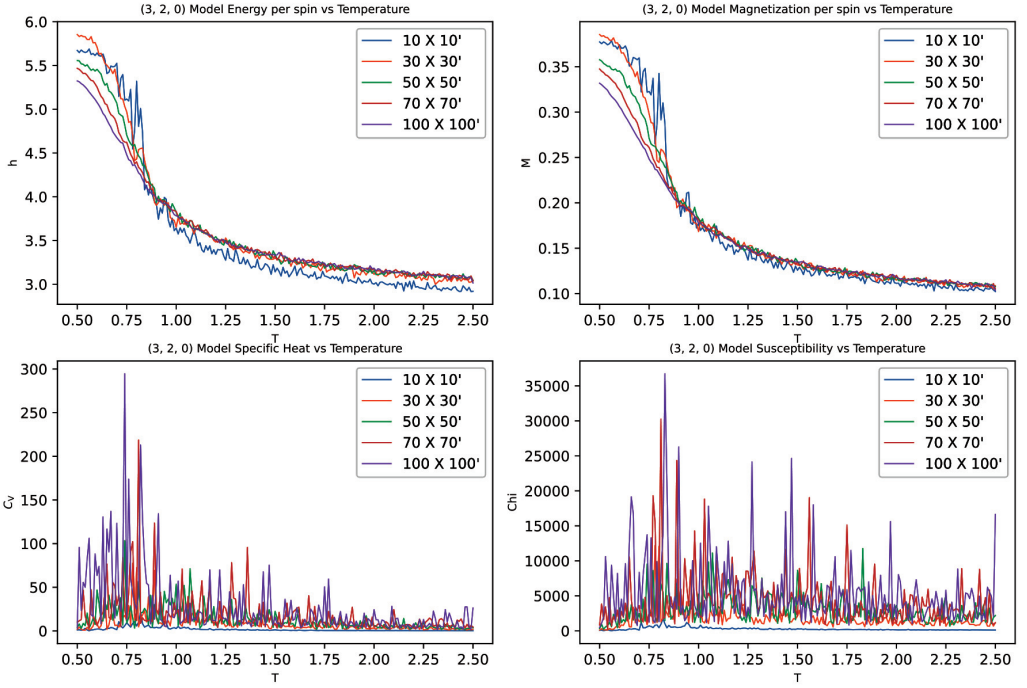

Figure 7: Graphs of observables $\langle O \rangle_{(3,2,0)}$ over temperature T for lattice size 10 × 10', 30 × 30', 50 × 50', 70 × 70' and 100 × 100'

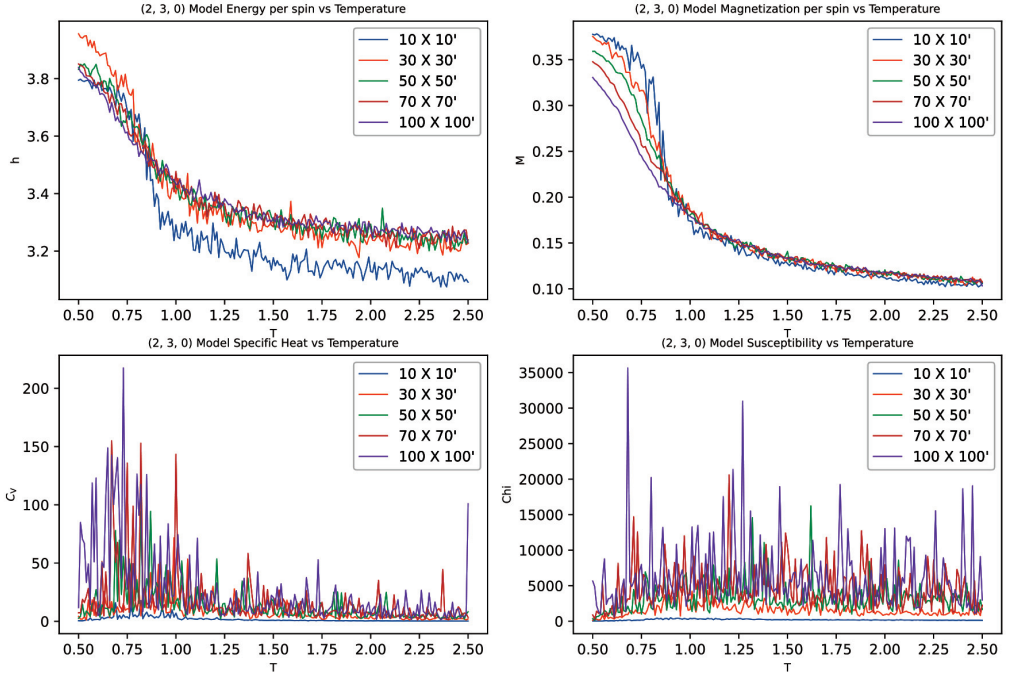

Figure 8: Graphs of observables $\langle O \rangle_{(2,3,0)}$ over temperature T for lattice size 10 × 10', 30 × 30', 50 × 50', 70 × 70' and 100 × 100'

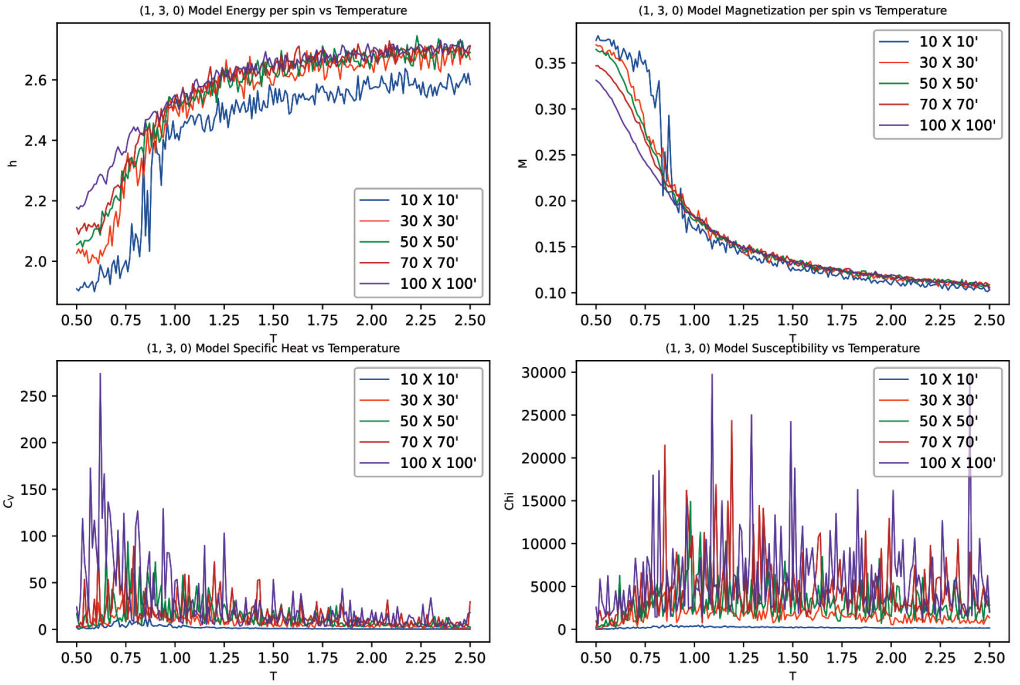

Figure 9: Graphs of observables $\langle O \rangle_{(1,3,0)}$ over temperature T for lattice size 10 × 10', 30 × 30', 50 × 50', 70 × 70' and 100 × 100'

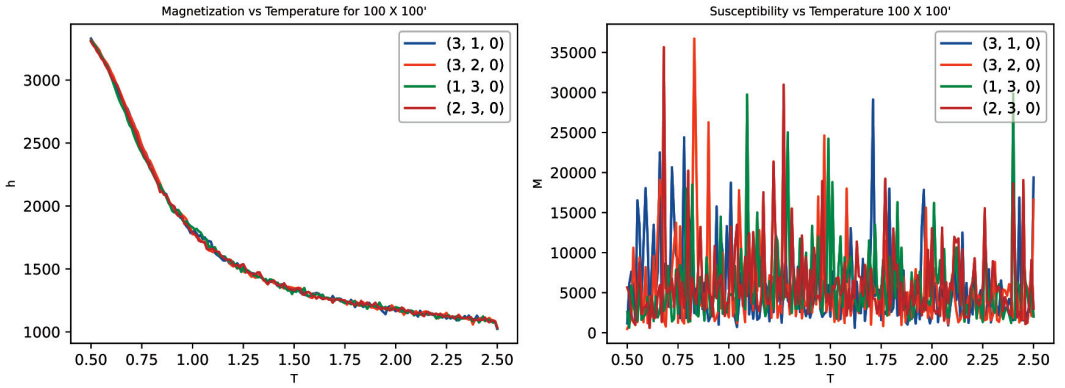

Figure 10: Graphs of magnetisation $\langle M_v \rangle$ and susceptibility $\langle \chi_s \rangle$ over temperature T for χ = (3, 1, 0), (3, 2, 0), (1, 3, 0), and (2, 3, 0)

Phase Transition(s) and Energy Level

Based on the observation from both the behaviour of the zeros of the partition function and observables from MCM simulation, it is suggested that the existence of the phase transition is visible in some cases. Other than this, Zakaria (2016) has proposed that the relations to their energy step could describe the existence of the phase transition(s) across models. Table 2 summarises the properties of each model and the observation of the phase transition(s) based on the zeros of partition functions and the graphs of the observables for each model.

In general, the result for every case suggests the existence of a phase transition. However, more evidence is necessary to deduce they have multiple phase transitions. Based on the observation from the zeros of partition function Z for the cases we studied, plus the instances of Z_5-symmetric model studied by Zakaria (2016), we can infer that the model with decreasing energy step is more stable and has a phase transition. In contrast, the model with increasing energy steps shows the possibility of multiple phase transitions, although they are prone to experience the finite size effect. Including the observation from the antiferromagnetic region can provide more information about the relationship between the energy step and the existence of the phase transition across model cases.

Another interesting observation is the summation of the subtraction of the energy list element. Here, we focused on the difference between $\chi[0]$ with other $\chi[i]$ as we study the ferromagnetic material. From Table 2, only the

Table 2: Properties and observation of phase transition(s) Z_5-symmetric models with χ = (3, 1, 0), (3, 2, 0), (1, 3, 0), and (2, 3, 0)

Properties	**(3, 1, 0)**	**(3, 2, 0)**	**(1, 3, 0)**	**(2, 3, 0)**
Energy step	(2, 1)	(1, 2)	(2, 3)	(1, 3)
$\sum_{0}^{2} \chi[0] - \chi[i]$	5	4	-1	1
Observed Range(s) of the critical point, T	(1.77, 2.26)	(1.72, 2.16)	(1.83, 2.37)	(1.44, 2.47)
	-	(1.96, 2.63)	-	-
Number of critical points, T	1	2	1	1

(1, 3, 0) case has negative summation and has decreasing total energy h. We could not estimate the range of the critical temperature T_c solely from the specific heat and susceptibility graphs as they were affected by a lot of noise. However, we can pinpoint the critical temperature T_c of the model based on the peak in the ranges that are obtained from the observation of the zeros. The estimation is shown in Table 2.

The specific heat graphs for all cases showed a more distinct peak for temperatures under 1. The peaks become sharper as the value of β increases rapidly. Hence, it is hard to determine the existence of phase transition at low temperatures. Nonetheless, further analysis using critical exponent values and scaling laws can give valuable information to estimate the critical temperature T_c. For this study, we depicted the system in the ferromagnetic and paramagnetic phases. A better definition of magnetisation that can capture other magnetic phases for the MCM simulation may give more evidence to the multiple-phase transitions.

Conclusions

We have studied the partition function and their zeros Z_5-symmetric models on the square lattice. The zeros are plotted in a complex Argand plane to study the analytical structure of the zeros distributions. Our research supports some relations regarding the comparison between the cases of Z_Q-symmetric model. We also provide another tool to study the Z_Q-symmetric model. Finding the range of the graphs' singularity is only the first step to support the claim that this structure suggests the behaviour of physical observables at thermodynamic limits related to phase transition. Further analysis of the results will give more insights. For the moment, although it is very interesting to extend the distribution of the zeros further to larger cases to predict the exact locus of zeros, the computing resources at hand are limiting our study. The implementation of parallel computing and cloud computing are the options for improvement. The study of cases with $\chi[0] = 0$ should be considered for future work to provide more insight into this model. Overall, the study of this more generalised model is vital to mimic the system in the real world as closely as possible to help the experimental works in a more sustainable approach.

Acknowledgements

The Ministry of Higher Education Malaysia financially supported this research under grant number FRGS/1/2022/STG06/UIAM/02/1.

Conflict of Interest Statement

The authors declare that they have no conflict of interest.

References

Diestel, R. (2006). *Graph theory,* (3rd ed.). Springer.

Eastman P. (2018). *Introduction to statistical mechanics*. Retrieved from https://web.stanford.edu/~peastman/statmech/

Einstein, A. (1905). Über die von der molekularkinetischen Theorie der Wärme geforderte Bewegung von in ruhenden Flüssigkeiten suspendierten Teilchen. *Annalen der Physik, 17*, 549-560.

Fisher, M. E. (1965). The nature of critical points. In W. E., Britten (Ed.)*, Lectures in theoretical physics* (7c, pp. 1-159). University of Colorado Press, Boulder.

Fisher, M. E. (1967). Finite-size effects in phase transitions, In W. E. Britton (Ed.), *Lectures in theoretical physics,* (6). University of Colorado Press, Boulder.

Ising, E. (1925). Beitrag zur Theorie des Ferromagnetismus. *Zeitschrift Für Physik, 31*(1), 253-258.

Kadanoff, L. P. (1966). Scaling laws for Ising models near T_c. *Physics, 2*, 263.

Kotze, J. (2008). Introduction to Monte Carlo methods for an Ising model of a ferromagnet. *arXiv.*

Kubo, R. (1966). The fluctuation-dissipation theorem. *Report on Progress in Physics, 29*, 255.

Manshur, N. S. M., Zakaria, S. F. & Ganikhodjaev, N. (2020). The Z_6-symmetric model partition functions on a triangular lattice. *Malaysian Journal of Fundamental and Applied Sciences*, *16*(3), 264-270.

Marsden, J. & Hoffman, M. (1999). *Basic complex analysis.* W. H. Freeman.

Martin, P. (1991). *Potts models and related problems in statistical mechanics*. World Scientific Publishing Company.

Metropolis, N., Rosenbluth, A. W., Rosenbluth, M. N., & Teller, A. H. (1953). Equation of state calculations by fast computing machines. *Journal of Chemical Physics, 21*(6).

Onsager, L. (1944). Crystal Statistics. I. A two-dimensional model with an order-disorder transition. *Physical Review, 65*, 117-149.

Papoulis, A. & Pillai, S. (2011). *Probability, random variables and stochastic process with Errata sheet.* McGraw-Hill Series in Electrical and Computer Engineering, McGraw-Hill.

Potts, R. B. (1952). Some generalized order-disorder transformations. *Mathematical Proceedings of the Cambridge Philosophical Society, 48*(1), 106-109.

Shackelford, J. F. (2000). *Introduction to Material Science for Engineers*. Prentice-Hall Inc, fifth edition.

Yang, C. N. & Lee, T. D. (1952). Statistical theory of equations of state and phase transitions I. Theory of condensation. *Physical Review*, *87*(3), 404-409.

Zakaria, S. F. (2016). *Analytic properties of Potts and Ising model partition functions and the relationship between analytic properties and phase transitions in equilibrium statistical mechanics*, Doctoral dissertation, University of Leeds.

Zakaria, S. F. & Manshur, N. S. M. (2019). The zeros distribution of the Z_5-symmetric model on a triangular lattice. *Malaysian Journal of Fundamental and Applied Sciences, 16*(3), 307-313.